Journal of the European Ceramic Society 23 (2003) 491–497

www.elsevier.com/locate/jeurceramsoc

Microstructural characterization of plasma-sprayed nanostructured zirconia powders and coatings

Huang Chen*, Yi Zeng, Chuanxian Ding

Shanghai Institute of Ceramics, Chinese Academy of Sciences, Shanghai, 200050, People's Republic of China

Received 15 November 2001; received in revised form 29 March 2002; accepted 11 April 2002

Abstract

The objective of this paper was to study the melting state of nanoscale zirconia powders in plasma jet, examine the crystalline phase and microstructural characterization of the plasma sprayed nanostructured zirconia powders and coatings. The cross-section morphology of water-quenched powders revealed that most of the starting powders were molten in the plasma jet. Phase analysis using XRD spectra proved that the monoclinic phase zirconia of the starting powders transferred into tetragonal phase zirconia after the plasma spraying. SEM analysis indicated that the as-sprayed coatings exhibited lamellar structure, about 0.5–5 μm in thickness of a single lamella, which was found to be a characteristic feature of the plasma-sprayed nanostructured zirconia coating. Inside of the lamellae, columnar grains were observed. The mean grain size of the as-sprayed zirconia coating is about 80 nm.

Keywords: Coatings; Microstructure; Plasma spraying; ZrO_2

1. Introduction

The preparation and characterization of nanostructured ceramic coating has become an active field.[1–3] Many techniques have been used to fabricate nanostructured ceramic coatings .[4–11] However, the way more likely to benefit is deposition of the coating by a thermally activated process, on the basis of successfully producing the nano-titanium oxide coating and nano-tungsten carbide coating in our previous works .[4,11] In recent years, the increasing potential of nanostructured zirconia ceramic coatings used as thermal protection and wear resistance has been focused on. It was reported that nanostructured thermal barrier coatings (TBCs) had the potentiality of improved durability and reduced thermal conductivity. The improvement of durability is due to the enhancement of "splat" boundary strength of coating and the decrease of thermal conductivity resulting from the reduction of grain size and the optimization pore size of the zirconia coating.[1,3,10]

In this paper, an interest has been taken in the melting state of nanostructured zirconia powders in plasma spraying and the microstructure of the nanostructured zirconia powders by water-quenched and as-sprayed coatings in order to understand the formation and properties of plasma sprayed nanostructured zirconia coating. The objective of this work was to examine the melting state and the phase transformation of nanoscale zirconia powders during the plasma spraying and to characterize the microstructures of zirconia powders and the as-sprayed coating.

2. Experimental method

The as-received nanoscale powders could not be used as feedstock to deposit nanostructured coatings during plasma spraying because of their bad flowability.[12,13] To overcome this problem, a commercial nano-zirconia (3 mol% Y_2O_3) powders were reprocessed through a spray drying process to form granules with sizes in the range of 15–40 μm in this experiment. The spray-dried granules were sprayed into distilled-water and deposited onto stainless-steel substrates located at 120 mm away from the plasma gun nozzle. The Metco A-2000 atmospheric plasma spraying equipment with F4-MB plasma

* Corresponding author. Tel.: +86-21-62512990; fax: +86-21-62513903.

E-mail address: chenhuang@citiz.net (H. Chen).

0955-2219/02/$ - see front matter
PII: S0955-2219(02)00096-1

gun (Sulzer Metco AG, Switzerland) was applied to deposit the samples. The feedstock powders were fed with a Twin-System 10-C (Plasma-Technick AG, Switzerland). The Ar–12% H_2 mixture was used as plasma forming gas. Prior to the spraying, the substrate was degreased ultrasonically in acetone and blasted with alumina grit. During spraying, the substrates and coatings were cooled using compressed air. The details of the sample preparation were described in our previous paper.[6]

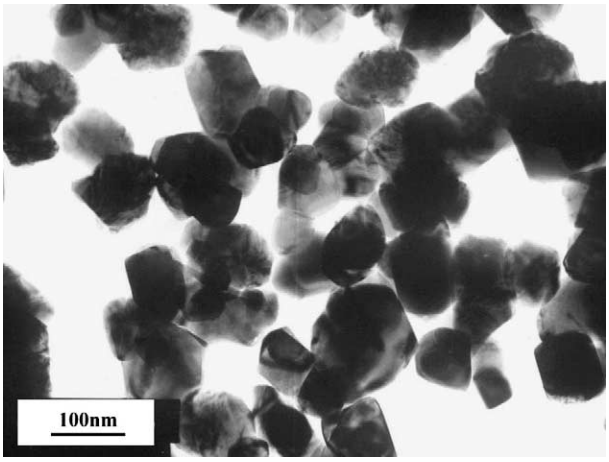

Fig. 1. TEM micrography of starting powder.

The phases of the powders and coatings were characterized by a RAX-10 X-ray diffractometer (Rigaku, Tokyo, Japan), using CuK_α radiation (40 kV, 100 mA). The morphologies of the as-sprayed coatings were observed with an EPMA-8705QH_2 electron probe analyzer (Shimadzu, Tokyo, Japan). The microstructure of powders and coatings were analysised by a JEM-200CX TEM (Jeol, Tokyo, Japan). The roughnesses of as-sprayed coatings were measured with 0.5 mm/s traverse speed at 4.8 mm length using a TK300 HOMMEL WERKE roughness tester (Wave, Germany).

3. Results and discussion

3.1. Characterization of starting powder

TEM micrography of the as-received nanoscale zirconia powders was shown in Fig. 1. It could be seen that the size of the powders was in the range of 50–120 nm. Selection electron diffraction (see Fig. 2) and X-ray diffraction pattern of the starting powders (see Fig. 3) revealed that the nanoscale powders were composed of tetragonal and monoclinic zirconia phases. Fig. 4 showed the morphology of spray dried zirconia powders

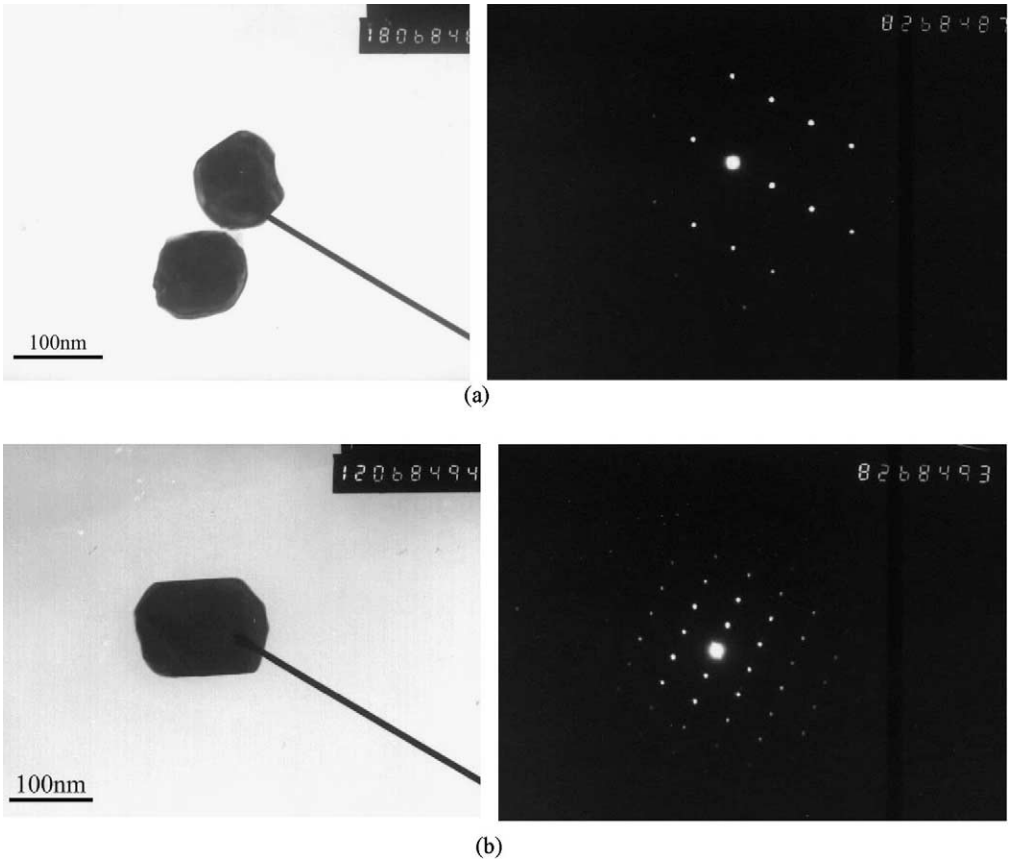

Fig. 2. SED of starting powder (a) tetragonal, (b) monoclinic.

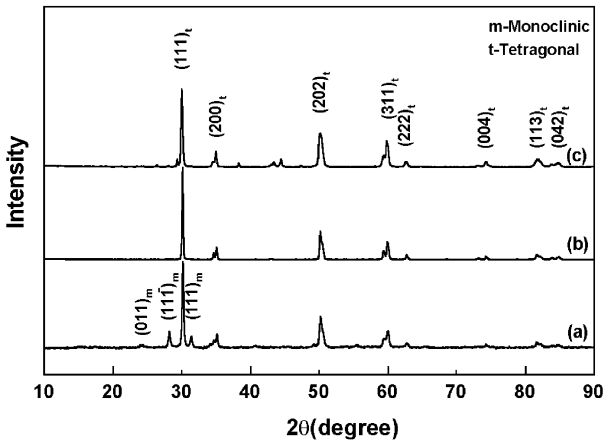

Fig. 3. X-ray diffraction patterns of (a) starting powder, (b) water-quenched powder, and (c) as-sprayed coating.

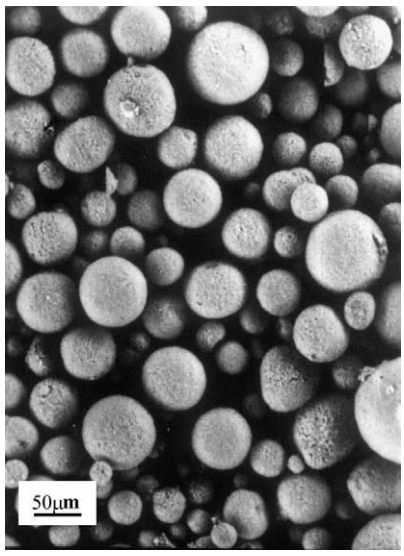

Fig. 4. The morphology of spray-dried zirconia powders.

that were spherical and spherical. The powder has excellent flowability and is suitable for plasma spraying.

3.2. Microstructural characterization of water-quenched sprayed powders

In order to examine the melting state of the nanoscale zirconia powders in the plasma jet, the powders were sprayed into distilled-water. SEM observation showed that the water-quenched powders displayed a ball-like microstructure with cellular-dendritic on the surface, which were shown in Fig. 5. It was reported[14] that the feedstock powders were melted and homogenized during the short residence time in the plasma jet. When the molten and semi-molten droplets of zirconia were injected into distilled-water, they experienced a very high cooling rate, thus the cellular-dendritic microstructure was formed as can be seen in Fig. 5. Compared with the surface morphology of starting feedstock powders as shown in Fig. 4, it was found that the powders quenched with distilled-water were smoother and denser. From the cross-section of water-quenched sprayed powders, as shown in Fig. 6, it can be seen that the starting powders were melted and a ball-like thin wall was formed during plasma spraying in spite of short residence time. The good melting may be due to the large specific surface and high active energy of the nanostructured material.[15] Some cracks and bright faint rings were presented in the cross-section of water-quenched powders. The cracks resulted from relaxation of heat stress and bright rings were due to porosity, which caused charge in the SEM observation.

Fig. 7 presented the TEM micrograph of the water-quenched powders. Two kinds of grains with different sizes can be seen in Fig. 7. One was about 50–120 nm in size, the other was in the range of 1–10 nm. The small grains were ball like. It was explained in terms of the nucleation crystallizing from the molten powders. In general, the nucleation had not enough time to grow due to the high cooling rate, so their sizes were very small. It was also noted that some grains grew unavoidably over 100 nm, which is because of their different thermal history during plasma spraying. It is believed

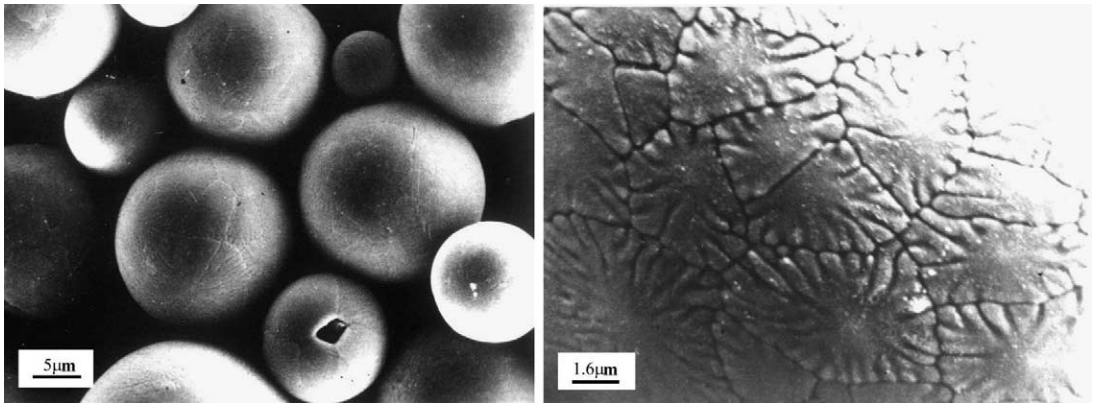

Fig. 5. The cellular-dendritic morphology of the plasma-melted and water-quenched zirconia powders.

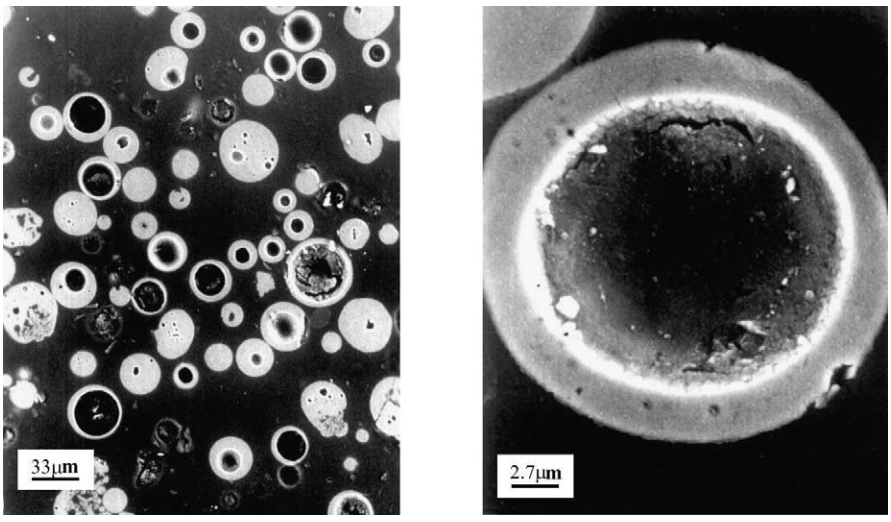

Fig. 6. The cross-section morphology of the plasma-melted and water-quenched zirconia powders.

that temperature differences of several hundred degrees may exist in the gas flow field.[16,17] The nanostructured grains in the as-sprayed coating were composed of the nanoscale grains crystallizing from the molten and semi-molten of the starting powders and the non-molten nanoscale grains.[18,19]

3.3. Phase analysis

XRD spectra of the starting powders, water-quenched powders and as-sprayed coating were shown in Fig. 3. From Fig. 3, it can be seen that the starting powders consisted of metastable tetragonal phases. A few of the monoclinic zirconia phases were also found in the XRD spectrum. After the plasma spraying, the peaks of monoclinic phase disappeared. These results indicated that the water-quenched powders and as-sprayed coatings were mostly composed of tetragonal phase zirconia. The phenomenon can be explained in terms of the melting and cooling of starting powders. During the plasma spraying, the powders experienced very high heating and cooling rate, which prevented the transformation of zirconia particles from the tetragonal phase to monoclinic phase.[19]

3.4. Microstructural characterization of coating

Fig. 8 presented the surface morphology of the as-sprayed zirconia coating. The surface of coating was smooth and its surface roughness Ra was about 5.9 μm, which was smaller than that of traditional counterparts sprayed at the same conditions.

Fig. 9 presented the fracture morphologies of as-sprayed nanostructured zirconia coating at different magnifications. These micrographs revealed that the plasma sprayed nanostructured zirconia coatings still

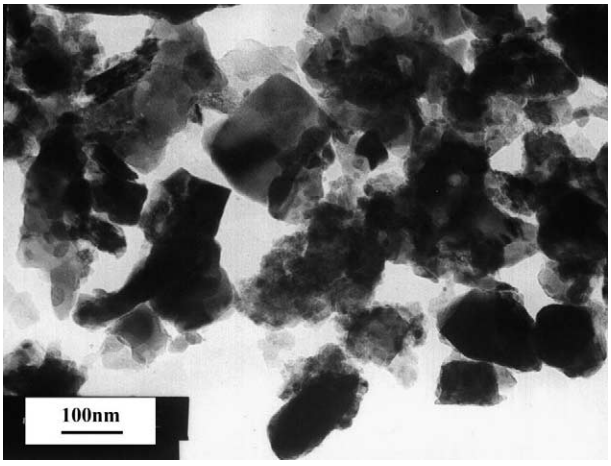

Fig. 7. TEM micrograph of water-quenched powders.

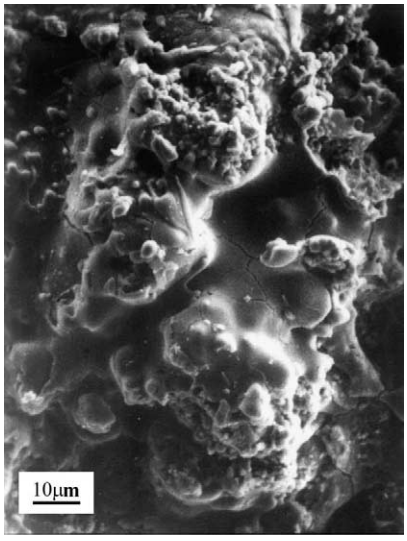

Fig. 8. Morphology of as-sprayed nanostructured zirconia coating.

exhibited the typical lamellar structure. The lamellae were invariably aligned parallel to the stainless-steel substrate and previously deposited material.[20] Some loose microstructure appeared in Fig. 9b, which resulted from the existence of the non-molten or semi-molten starting powders. The loose structure decreased the cohesive strengths between lamella. In addition, interlamellar porosity was seen in the fracture surface of the as-sprayed coating. It was believed to arise from the entrapment of the air during the plasma spraying.[8] Weak interlamellar cohesion existed due to the interlamellar porosity. This fracture morphology also indicated that solidification occurred in a discontinuous manner, deposited material completely solidifying to form the lamella prior to the impact of subsequent material, as interdiffusion had not been observed between lamellae.

The lamellar and columnar structures of individual platelets were clearly observed in Fig. 9c and d. Lamellar dimensions vary from about 5 μm thick towards the center to less than 0.5 μm at the periphery. The length of the lamella can extend up to about 120 μm. The length of individual lamella is often restricted by the topography of previously deposited materials. The results of the observation above was explained in terms of the good melting of starting powders, which led to the good deformation (flattening) when they impacted the stainless-steel substrates. As a result, the number of contact points increased and the cohesion between particles enhanced.[13] Inside of the lamella, the columnar

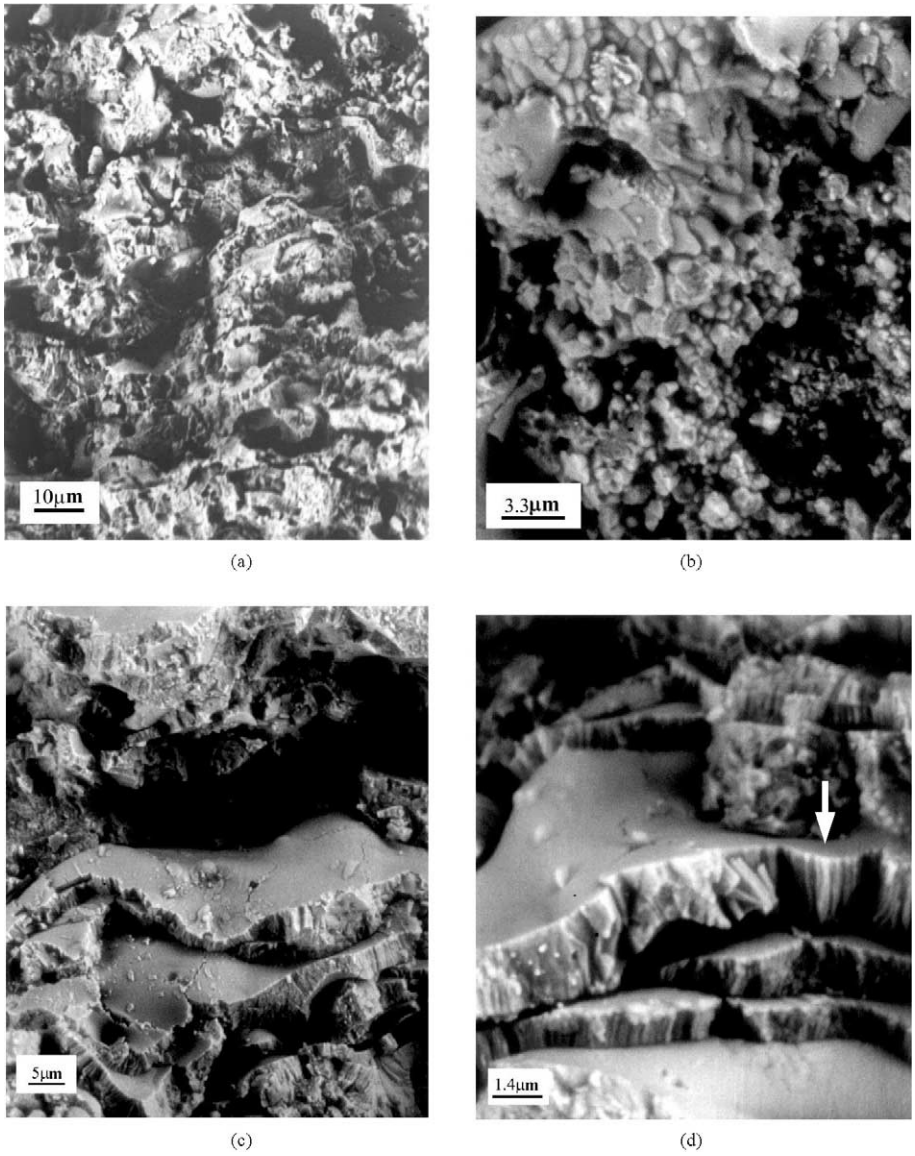

Fig. 9. Scanning electron micrographs of the fracture surface, (a) a typical micrograph of the fracture surface, (b) some loose microstructure in coating, (c) and (d) high magnification showing single lamellar structure.

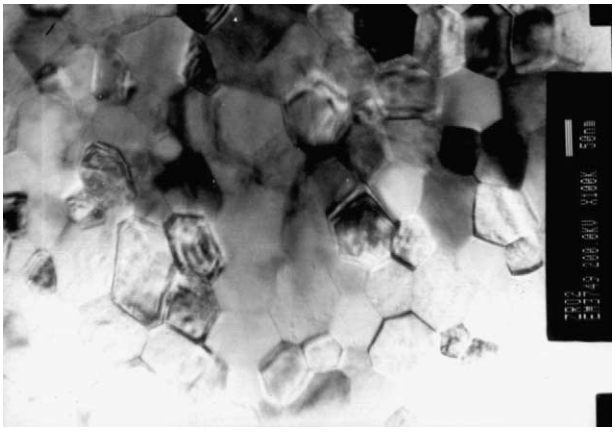

Fig. 10. TEM micrograph of the as-sprayed nanostructured zirconia coating.

grains were found as shown in Fig. 9d, and the diameters of columnar grains were about 0.05–0.3 μm. The arrow in Fig. 9d indicated the direction of columnar grain perpendicular to the substrate by and large. The lamellar microstructure was believed to be determined by the rate and direction of greatest heat removal from the deposited materials and its mode of crystallization.[19] Columnar grain growth in coating arises from heterogeneous nucleation at splat boundary and rapid growth into the molten splat.[20] The temperature gradient existing in the gas flow also causes the columnar grain growth throughout the thickness of the splat.[21] Alternatively fine equiaxed grains were formed as a result of homogeneous nucleation and precipitation from an undercooled melt as shown in Fig. 10. The estimated cooling rate of plasma-sprayed coating is up to 10^6 K/s.[5,20] It is well known that homogeneous nucleation resulted in the formation of fine grains (<0.1 μm diameter) due to the high nucleation and low growth rate. A reduction in the cooling rate results in a lower driving force for nucleation, which promoted grain growth.[20]

The degree of splat spreading and variation in lamellar thickness are controlled by a number of factors, such as temperature and viscosity of droplet, velocity of impact and wetting behaviour between the splat and the previously deposited material.[19,22] The thickness of each lamella is therefore dependent upon the amount of molten splat spread across the uneven surface prior to solidification. Lamellae are generally thicker at their center and thinner at their periphery with the shape dependent on the flow pattern of the molten material on impact.

A typical microstructure of the as-sprayed nanostructured zirconia coating was shown in Fig. 10. From Fig. 10, it can be seen that the as–sprayed zirconia coating is composed of fine equiaxed grains ranging from 30 to 110 nm and the mean grain size is about 80 nm. It is noticed that the average grain size of the as-sprayed coating is similar to that of the starting powders. However, the grain boundaries of the as-sprayed zirconia coating are clearer than those of the starting powder particles (Fig. 1). The formation of nanostructured in the plasma sprayed zirconia coating was explained in terms of the high temperature of plasma flame, short residence time in the plasma jet and high cooling velocity of the powder particles.[1,4,22]

4. Conclusions

1. Nanostructured zirconia coatings were deposited by atmospheric plasma spraying (APS). The mean grain size of the as-sprayed coatings is about 80nm, which is similar to that of starting nanoscale powders.
2. Due to the high cooling rate of the starting powders experienced in the distilled water, the cellular-dendritic microstructure was formed on the surface of water-quenched powders.
3. Fracture morphology of water-quenched powders showed that most of the starting powders were molten in the plasma jet in spite of short resistance time.
4. XRD spectra of the starting powers, water-quenched powders and as-sprayed coating indicated that water-quenched powders and as-sprayed coatings were composed of tetragonal zirconia phase. It is due to the good melting of starting powders and short residence time in plasma jet.
5. SEM analysis showed that the as-sprayed coatings had lamellar structure, about 0.5–5 μm from periphery to center, which indicated that nanostructured coating had better flattening than traditional coating. The solidification of splat appeared in a discontinuous manner. Inside of lamella, columnar grains were observed.

Acknowledgements

The authors would like to thank Mrs. Xiaming Zhou for the specimen preparation and Mrs. Jianhua Gao for the samples examination.

References

1. Berndt, C. C., Thermal spray processing of nanoscale materials II—extended abstracts. *J. Thermal Spray Technol.*, 2001, **10**(1), 147–181.
2. Gell, M., Application opportunities for nanostructured materials and coatings. *Mater. Sci. Eng.*, 1995, **A204**, 246–251.
3. Gell, M., The potential for nanostructured materials in gas turbine engines. *Nanostructured Mater.*, 1995, **9**, 997–1000.

4. Zhu, Y., Huang, M., Huang, J. and Ding, C., Vacuum-plasma sprayed nanostructured titanium oxide films. *J. Thermal Spray Technol.*, 1999, **8**(2), 219–222.
5. Zeng, Y., Lee, S. W., Gao, L. and Ding, C. X., Atmospheric plasma sprayed coatings of nanostructured zirconia. *J. Eur. Ceram. Soc.*, 2002, **22**, 347–351.
6. Chen, H. and Ding, C. X., Nanostructured zirconia coating prepared by atmospheric plasma spraying. *Surf. Coat. Technol.*, 2002, **150**, 31–36.
7. Shukla, V., Elliott, G. S. and Kear, B. H., Nanopowder deposition by supersonic rectangular jet impingement. *J. Thermal Spray Technol.*, 2000, **9**(3), 394–398.
8. Jordan, E. H., Gell, M., Sohn, Y. H., Goberman, D., Shaw, L., Jiang, S., Wang, M., Xiao, T. D., Wang, Y. and Strutt, P., Fabrication and evaluation of plasma sprayed nanostructured alumina-titania coatings with superior properties. *Mater. Sci. Eng.*, 2001, **A301**, 80–89.
9. Limsa, R. S., Kucuk, A. and Bernd, C. C., Integrity of nanostructured partially stabilized zirconia after plasma spray processing. *Mater. Sci. Eng.*, 2001, **A313**, 75–82.
10. Karthikeyan, J., Berndet, C. C., Tikkanen, J., Reddy, S. and Herman, H., Plasma spray synthesis of nanomaterial powders and deposits. *Mater. Sci. Eng.*, 1997, **A238**, 275–286.
11. Zhu, Y., Yukimura, K., Ding, C. and Zhang, P., Tribological properties of nanostructured and conventional WC-Co coatings deposited by plasma spraying. *Thin Solid Films*, 2001, **388**, 277–282.
12. Shaw, L. L., Goberman, D., Ren, R., Gell, M., Jiang, S., Wang, Y., Xiao, T. D. and Strutt, P. R., The dependency of microstructure and properties of nanostructured coatings on plasma spray conditions. *Surf. Coat. Technol.*, 2000, **130**, 1–8.
13. Lima, R. S., Kucuk, A. and Berndt, C. C., Evaluation of microhardness and elastic modulus of thermally sprayed nanostructured zirconia coatings. *Surf. Coat. Technol.*, 2001, **135**, 166–172.
14. Kear, B. H., Kalman, Z., Sadangi, R. K., Skandan, G., Colaizzi, J. and Mayo, W. E., Plasma-sprayed nanostructured Al_2O_3/TiO_2 powders and coatings. *J. Thermal Spray Technol.*, 2000, **9**(4), 483–487.
15. Kear, B. H. and Strutt, P. R., Chemical processing and application for nanostructured materials. *Nanostructured Mater.*, 1995, **6**, 227–236.
16. Fincke, J. R., Haggard, D. C. and Swank, W. D., Particle temperature measurement in the thermal spray process. *J. Thermal Spray Technol.*, 2001, **10**(2), 255–266.
17. Ahmed, I. and Bergman, T. L., Thermal modeling of plasmas spray deposition of nanostructured ceramics. *J. Thermal Spray Technol.*, 1999, **8**(2), 315–322.
18. Mcpherson, R., The relationship between the mechanism of formation, microstructure, and properties of plasma sprayed coatings. *Thin Solid Film*, 1981, **81**, 297–310.
19. Harmsworth, P. D. and Stevens, R., Microstructure of zirconia-yttria plasma-sprayed thermal barrier coatings. *J. Mater. Sci.*, 1992, **27**, 616–624.
20. Mcpherson, R., On the formation of thermally sprayed alumina coatings. *J. Mater. Sci.*, 1980, **15**, 3141–3149.
21. Bengtsson, P. and Johannesson, T., Characterization of microstructural defects in plasma-sprayed thermal barrier coatings. *J. Thermal Spray Technol.*, 1995, **4**(3), 245–251.
22. Sampath, S. and Herman, H., Rapid solidification and microstructure development during plasma spray deposition. *J. Thermal Spray Technol.*, 1996, **5**(4), 445–456.